Minimising Crosstalk in Microchannel Free-Space Optical Interconnects with the Presence of Higher Order Modes

Feng-Chuan F. Tsai, Christopher J. O'Brien, Aleksandar D. Rakić
School of Information Technology and Electrical Engineering, The University of Queensland, Brisbane QLD 4072, Australia

ABSTRACT

We investigate the combined effect of the diffraction-caused crosstalk noise (DCCN) and the stray-light crosstalk noise (SLCN) on the performance of FSOI system. A numerical simulator was employed in this study to investigate OI channel design. We determine that there exists an optimal focal length, which maximises the signal-to-noise ratio (SNR) by minimising the combined effects of DCCN and SLCN. For the fundamental mode, the optimal focal length is approximately 750μm; for both LG_{01} and LG_{10} modes, the optimal focal length occurs between f = 650 μm and f = 700 μm, depending on the interconnection distance and array pitch.

Keywords: Stray light crosstalk, free space optical interconnect, diffraction

1. INTRODUCTION

Performance requirements of short-distance digital communication links have increased because of the escalating demand for high speed and high density data links. However, large scale electronic systems are suffering from an interconnection bottleneck due to the inherent inductance and capacitance of electric interconnects. The most noticeable limitations are pin congestion, clock skew and bandwidth limitations [1, 2]. The high aggregate bandwidth and channel density achievable by optical interconnects (OIs) make them an ideal replacement for electrical interconnection schemes. Optical interconnects potentially have low power consumption, and can facilitate the development of novel designs for VLSI architectures, including heterogeneous multiprocessor systems and highly parallel computing systems [3-5]. Recent developments in the integration of Vertical-Cavity Surface-Emitting Laser (VCSEL) arrays and photodetector arrays with CMOS electronic circuitry have increased the practical potential of optical interconnects [6, 7].

Free-space optical interconnects (FSOIs) offer solutions for both chip- and board-level interconnection. Several OI designs based on two dimensional VCSEL arrays have been proposed [8-13]. From these studies, it is evident that one of the major factors determining the maximum channel density and bit-error ratio is the optical crosstalk noise within the system. The majority of proposed OI designs employ microlenses and other small-diameter optical elements to produce compact optical systems (microchannel architecture). Through miniaturisation, the microlens diameter will be decreased to allow for higher channel density, and the performance of the system will become increasingly dominated by diffraction.

The generic implementation of a parallel FSOI system consists of two microlens arrays, employed to collimate and focus the laser beams onto an array of photodetectors. The optical power which is correctly transmitted to its intended receiver is the signal, and the portion of the beam that trespasses on neighbouring channels is the crosstalk noise. The two main types of crosstalk mentioned in the literature are the diffraction-caused and stray-light crosstalk noise. Following a number of studies [14-16], diffraction-caused crosstalk noise is modelled as the power incident on unintended receiver microlenses due to diffraction at the transmitter microlenses and the spread of the laser beam between the transmitter microlens array and the receiver microlens array. Stray-light crosstalk noise [17] is the fraction of the emitted power imaged by the neighbouring transmitter microlens to other channels, possibly far from the intended one.

This paper investigates the effects of both forms of crosstalk noise on the performance of FSOI system. Although both types of crosstalk are related to the finite aperture of the transmitter and receiver microlenses, they behave very differently with respect to the FSOI design parameters. While most of the published studies discussing the issue of crosstalk consider the fundamental mode alone, the presence of higher order transverse modes will enhance the effect of

Photonics Packaging, Integration, and Interconnects VII, edited by Allen M. Earman, Ray T. Chen
Proc. of SPIE Vol. 6478, 64780B, (2007) · 0277-786X/07/$18 · doi: 10.1117/12.699804

both types of crosstalk, stray-light crosstalk noise in particular. In practice VCSELs tend to operate in several transverse modes simultaneously.

In this study, a numerical simulator was employed to investigate OI channel design. In our recent paper [18], we have shown that by altering array geometry, the overall SNR can be improved. Extending from the recent paper, we demonstrate that there exists an optimal focal length which maximises the SNR by minimising the combined effects of diffraction-caused and stray-light crosstalk. In Sec. 2, the FSOI simulation model is developed. Experiments are performed on a commercial oxide-confined VCSEL to determine the modal content of the VCSEL beam, Sec. 3. These experimental findings are used to compare diffraction-caused and stray-light crosstalk in Sec. 4. A simple and accurate behavioural model for stray-light crosstalk is proposed in Sec. 5, and the paper is concluded with a brief discussion in Sec. 6.

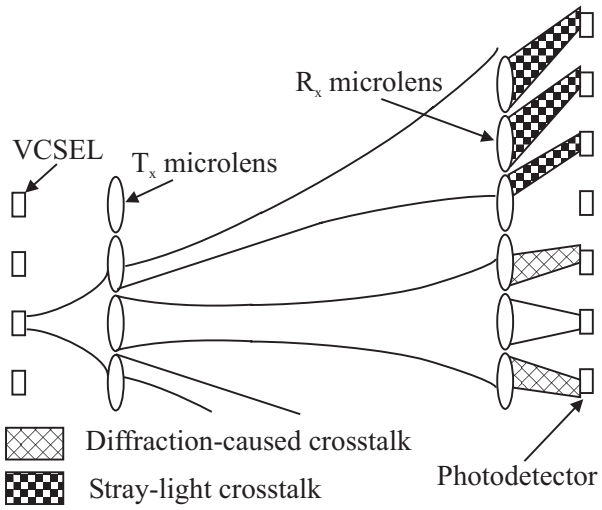

Figure 1: The schematic of free-space optical interconnect showing the diffraction-caused and stray light crosstalk

2. FSOI SIMULATION MODEL DESCRIPTION

2.1 Diffraction-caused crosstalk

For each channel, we consider a laser beam of beam waist ω_0, emitted from the transmitter plane through its corresponding transmitter microlens and imaged to an intermediate beam waist. The beam propagates from the intermediate beam waist to the intended receiver microlens. Due to diffractive spreading, the beam radius at the receiver microlens frequently exceeds the radius of the receiver microlens. Therefore, a fraction of the transmitted power will fall on the microlenses adjacent to the intended microlens, and will be focussed onto unintended photodetectors, Fig. 1, introducing crosstalk noise. This noise is typically assumed to be the dominant component of the optical crosstalk noise. In this article we will refer to it as the diffraction-caused crosstalk noise (DCCN). The DCCN is defined as the optical power that propagates through the intended transmitter microlens, but falls onto an adjacent receiver microlens and is focussed onto photodetectors for which it was not intended.

2.2 Stray-light crosstalk

We now consider another source of optical crosstalk, introduced by [17]. Again, we consider an arbitrary channel within the microchannel architecture, depicted by Fig 1. In this case, we concentrate on the fraction of power emitted by the VCSEL that falls on the transmitter microlenses adjacent to the intended transmitter lens. Due to the curvature of the microlenses, the beam is refracted away from the intended channel as shown in Fig 1. As it propagates through the channel, the beam will further expand until it reaches the receiver microlens plane. Unlike the diffraction-caused crosstalk, where most of the noise can be attributed to the adjacent channels, the beam can be redirected to photodetectors far from the intended channel. Therefore, in our simulations we depart form the usual analysis in which a

channel will only contribute noise to its nearest neighbours. In this study we demonstrate that, once stray-light crosstalk is properly accounted for, significant crosstalk can be introduced to a receiver by non-neighbouring channels. This type of crosstalk, caused by the overfill of the transmitter microlens, will be referred to as stray-light crosstalk noise (SLCN) throughout this article.

To calculate the crosstalk noise present in the central channel, we consider the noise induced on a central photodetector by all the channels surrounding it. However, the same result can be obtained by calculating the optical power falling on the surrounding photodetectors from the central channel. In this manner, the computational complexity of calculating the signal and noise powers can be greatly reduced by considering the transmission of a single beam over a large area, instead of the propagation of a large number of beams into a localised area.

2.3 Design Outline

Figure 1 shows the basic architecture used in the simulations: a microchannel FSOI constructed from two microlens arrays, a VCSEL array, and a photodetector array. The VCSEL array is located at $z = 0$, and the first microlens array is situated at $z = d_1$. The second microlens array is at a distance of $d_2 + d_3$ away from the first microlens array, and the photodetector array is positioned $d_4 = d_1$ away from the second microlens. The pitch of the array is Δ, and the diameter of the microlens is D. The fill factor, β, is defined as the ratio of the microlens diameter to the array pitch: $\beta = D/\Delta$. Two metrics frequently used to assess interconnect performance are the maximum achievable channel density, $1/\Delta^2$, and the interconnect length, $L = d_1+d_2+d_3+d_4$.

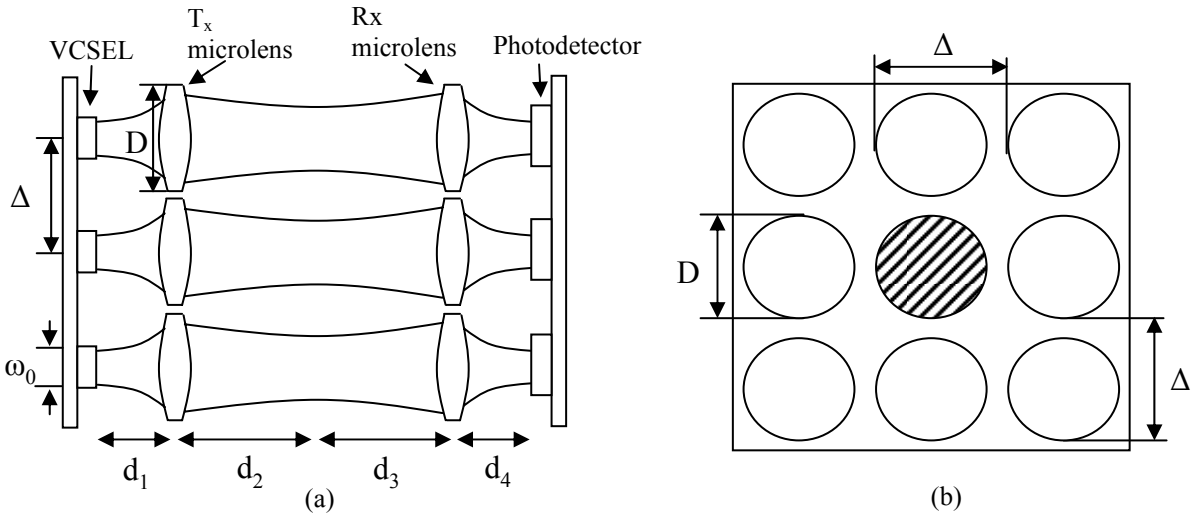

Figure 2: (a) Schematic of a microchannel free-space optical interconnect. (b) Structure of the T_x or R_x microlens array with x-y axis.

3. EXPERIMENTAL MEASUREMENT OF HIGHER ORDER TRANSVERSE MODES

For drive currents above threshold, VCSELs typically operate simultaneously in several higher-order transverse modes. In addition to lasing at a slightly different wavelength, these transverse modes propagate with a larger spot size than the fundamental mode and diverge more quickly. The modal composition of a VCSEL is, therefore, an important consideration when attempting to calculate the crosstalk noise in an optical interconnect.

The beam profiles of the transverse modes can be described by two families of orthogonal solutions to the paraxial wave equation: the Hermite-Gaussian (HG) and Laguerre-Gaussian (LG) modes. The LG profiles, expressed in cylindrical coordinates, are the most appropriate representation for our purposes and are presented below [19]:

$$\begin{Bmatrix} \psi_{nm}(r,\theta,z) \\ \psi_{nm}^{*}(r,\theta,z) \end{Bmatrix} = K_{nm}\left(\frac{r\sqrt{2}}{w(z)}\right)^{m} L_n^{(m)}\left(\frac{2r^2}{w(z)^2}\right)\exp\left(\frac{-r^2}{w(z)^2} - j\frac{kr^2}{2R(z)}\right)\begin{Bmatrix} \cos(m\theta) \\ \sin(m\theta) \end{Bmatrix} \quad (1)$$

where,

$$K_{nm} = A_{nm} N_{nm} \tag{2}$$

and,

$$A_{nm} = \exp\left\{ j\left[(2n+m+1)\arctan\frac{\lambda(z-z_s)}{\pi w_s{}^2} - k(z-z_s) \right] \right\} \tag{3}$$

and,

$$N_{nm} = \frac{2}{w(z)\sqrt{\pi(1+\delta_{om})}} \left[\frac{n!}{(n+m)!} \right]^{1/2}. \tag{4}$$

In the above equations, the wave number is $k = 2\pi/\lambda$, and the Rayleigh range is given as $z_R = \frac{1}{2} k\, w_s{}^2$, where w_s is the beam waist and is located at $z = z_s = 0$. The beam radius at any distance along the propagation axis is given as:

$$w(z) = w_s \sqrt{1 + \left(\frac{z}{z_R} \right)^2}\ , \tag{5}$$

and the radius of curvature is

$$R(z) = z\left[1 + \left(\frac{z_R}{z} \right)^2 \right]. \tag{6}$$

Equation (3) shows the Guoy phase shift experienced by the laser beams. Higher-order modes (n, $m > 0$) will experience a greater phase shift than the fundamental Gaussian mode, and will resonate at shorter wavelengths inside a cavity. This explains the spectral separation of transverse modes in a laser.

In order to examine the effect of transverse modes, it is necessary to determine the modal content of practical devices. Experiments were performed on a commercially available VCSEL (*Mode 8085-2008*). The continuous-wave, room temperature optical spectra were measured at drive currents up to $7 \times I_{th}$, at intervals of 0.05 mA. From this data, the evolution of the VCSEL spectrum was examined and a modally resolved light-current curve was constructed.

The presence and relative power of higher order modes can be observed from the optical spectra,, but their spatial profiles can not be identified. To accomplish this, an actuator controlled fibre probe was used to scan a cross section of the magnified near field of the laser beam. At each point of a 15×15 grid, the spectrum was recorded, and the modal peaks were isolated. From these measurements, we determined the optical power associated with each mode at each spatial pixel. The dominant lasing modes of this VCSEL can be identified as LG_{00}, LG_{01} and LG_{10}, shown in Fig. 3.

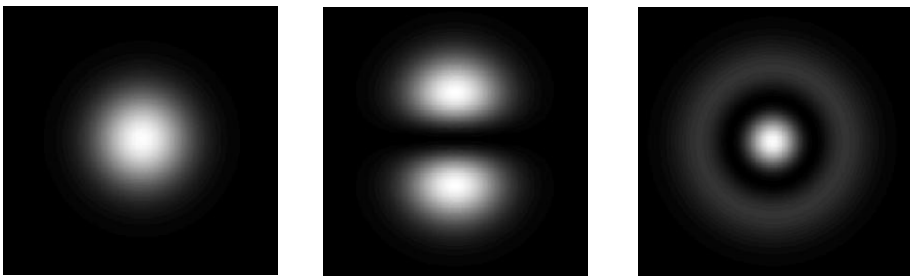

LG_{00} LG_{01} LG_{10}

Figure 3: Mode patterns of Laguerre-Gaussian modes

4. SIMULATION RESULTS

Commercial simulation software (Code V) is used to simulate the SLCN and DCCN. The design parameters used for simulation are as follows: the pitch between the channels is 250 μm, the beam has a waist radius of 3 μm and a central wavelength of 850 nm. The transmitter and receiver microlenses are assumed to be spherical lenses, made from BK7 optical glass, with a 95% fill factor. The focal length of all microlenses is 800 μm and the distance between the VCSEL and the transmitter microlens is fixed at $d_1 = f + z_R$, where f is the microlens focal length, and z_R is the Rayleigh range. The simulation was performed on a lattice microlens array of 64×64 channels. The crosstalk noise is measured by the optical power incident upon unintended receiver microlenses. The SNR is defined by

$$SNR = 10\log_{10}\frac{S}{SLCN + DCCN} \tag{7}$$

where S is the normalized optical power received by the corresponding photodetector.

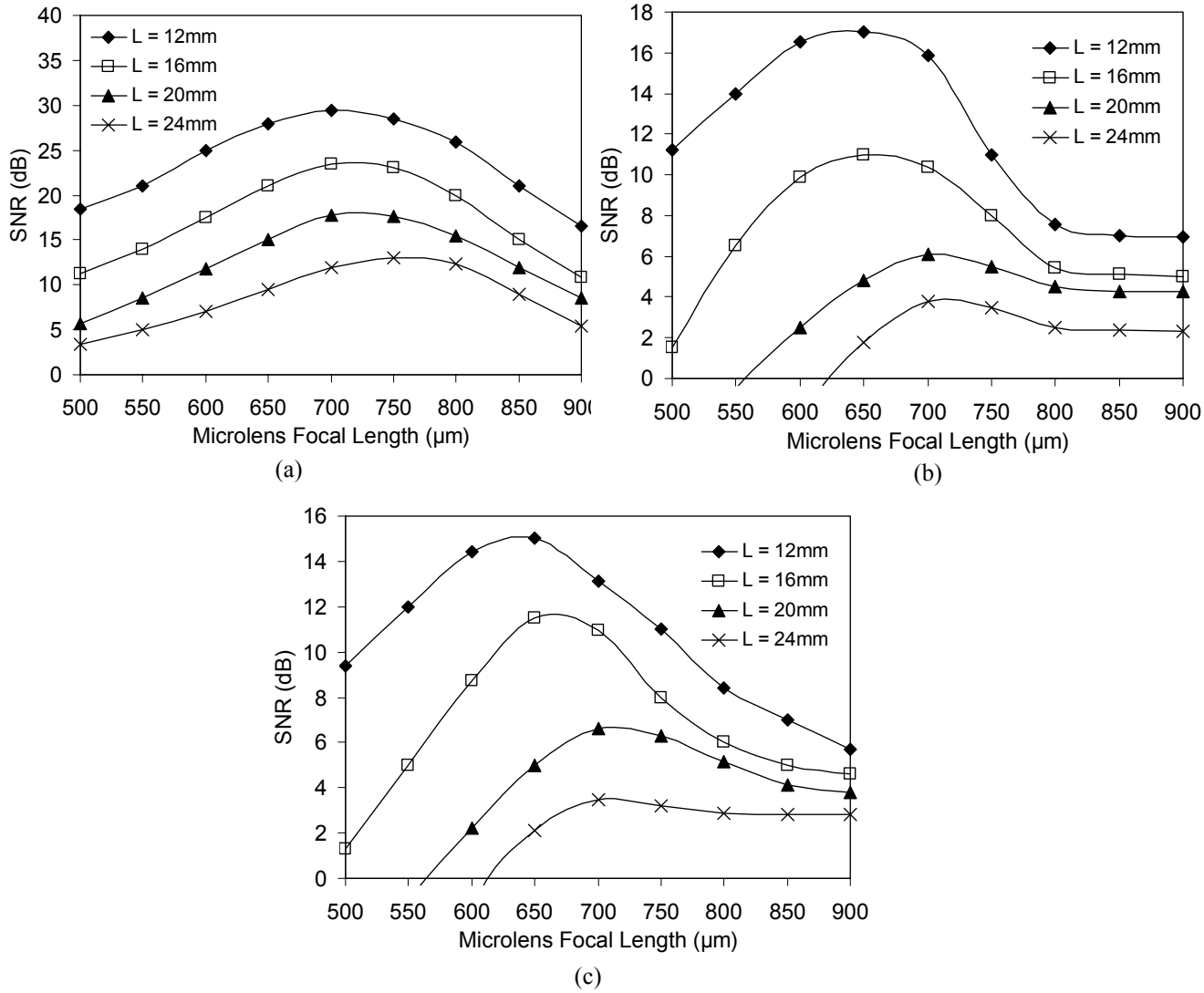

Fig. 4: Interconnect SNR with increasing microlens focal length for different interconnection distance
(a) LG_{00} mode (b) LG_{01} mode (c) LG_{10} mode

Optical interconnect designs are typically evaluated by considering the propagation of point sources or from the uniform surface emitters. To determine the effect of higher order transverse modes on FSOI performance, we propagate a two-dimensional beam profile through the optical system. The extended sources used in these simulation are formed from the weighted combination of Laguerre-Gaussian modes, determined experimentally in sec. 3: LG_{00}, LG_{01} and LG_{10}, Fig 3. The transverse profile is mapped onto a 101×101 point computational grid used as the beam definition for the diffraction-based beam propagation. A combination of geometrical ray tracing and diffraction-based propagation techniques are used to trace the beam through the optical interconnect.

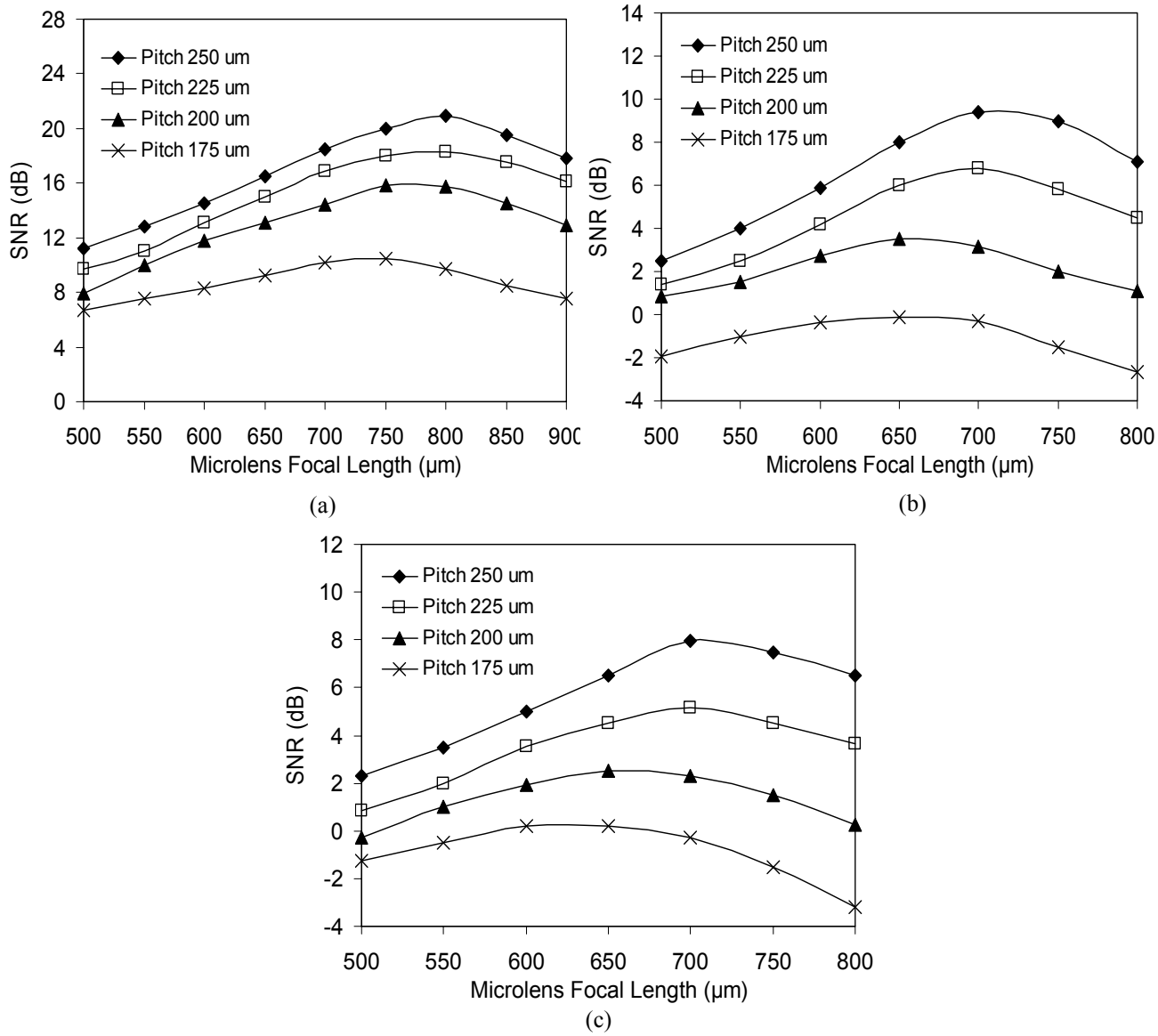

Fig. 5: Interconnect SNR with increasing microlens focal length for different system pitch
(a) LG_{00} mode (b) LG_{01} mode (c) LG_{10} mode

Figure 4 shows the interconnect SNR with increasing microlens focal length for different interconnect distance. By varying the microlens focal length between 500 μm and 900 μm we swept the FSOI operating regime from virtually "zero" beam clipping (at f = 500 μm) to substantial clipping at f = 900 μm. The results for the LG_{00}, LG_{01} and LG_{10} modes are shown in Figs. 4(a), 4(b) and 4(c) respectively. It can be seen that as the interconnection distance increases,

the optimal microlens focal length shifts higher for all transverse modes. The LG_{00} mode exhibits a prominent maximum between f = 700 μm and f = 750 μm depending on the interconnect distance. On the other hand, LG_{01} and LG_{10} modes have a maximum SNR at shorter microlens focal length of between f = 650 μm and f = 700 μm.

Figure 5 shows the interconnect SNR with increasing microlens focal length for different system pitch. The interconnection distance of 20 mm was used. Again, the microlens focal length value was varied between 500 μm and 900 μm and the results for the LG_{00}, LG_{01} and LG_{10} modes are shown in Figs. 5(a), 5(b) and 5(c) respectively. It can be observed for all modes that as the system pitch decreases, the maximum SNR will shift to a shorter microlens focal length. For LG_{00} mode, the maximum takes place between f = 750 μm and f = 800 μm; the maximum SNR for LG_{01} and LG_{10} modes occurs at a shorter focal length, between f = 650 μm and f = 700 μm.

5. CONCLUSION

We have demonstrated that there exists an optimal focal length which maximises the SNR by minimising the combined effects of diffraction-caused and stray-light crosstalk noise. For LG_{00}, the optimal focal length is around 750μm and for both LG_{01} and LG_{10} modes optimal focal length occurs between f = 650 μm and f = 700 μm depend on the interconnection distance and array pitch. For all modes, it can be seen that the optimal microlens focal length shifts higher for longer interconnects. As the system pitch decreases, the maximum SNR will shift to a shorter microlens focal length.

REFERENCES

1. D. A. B. Miller, "Invited paper: Physical reasons for optical interconnection," International Journal of Optoelectronics Vol. 11, pp. 155-168, 1997.
2. D. A. B. Miller, “Rationale and challenges for optical interconnects to electronic chips,” Proceedings of IEEE, Vol. 88, pp. 728-749, 2000.
3. D. V. Plant and A. G. Kirk, "Optical interconnects at the chip and board level: challenges and solutions," Proceedings of IEEE, Vol. 88, pp. 806-818, 2000.
4. D. Fey, W. Erhard, M. Gruber, J. Jahns, H. Bartelt, G. Grimm, L. Hoppe, and S. Sinzinger, "Optical interconnects for neural and reconfigurable VLSI architecture," Proceedings of IEEE, Vol. 88, pp. 838-847, 2000.
5. N. McArdle, M. Naruse, H. Toyoda, Y. Kobayashi, and M. Ishikawa, "Reconfigurable Optical Interconnections for Parallel Computing," Proceedings of IEEE, Vol. 88, pp. 829-837, 2000.
6. K. M. Geib, K. D. Choquette, D. K. Serkland, A. A. Allerman, and T. W. Hargett, "Fabrication and performance of two-dimensional matrix addressable arrays of integrated vertical-cavity lasers and resonants cavity photodetectors," IEEE Journal of Selected Topics in Quantum Electronics, Vol. 8, pp. 943-947, 2002.
7. R. H. Havemann and J. A. Hutchby, "High-Performance Interconnects: An Integration Overview," Proceedings of IEEE, Vol. 89, pp. 586-601, 2001.
8. M. Châteauneuf, A. G. Kirk, D. V. Plant, T. Yamamoto, and J. D. Ahearn, "512-channel vertical-cavity surface-emitting laser based free-space optical link," Applied Optics, Vol. 41, pp. 5552-5561, 2002.
9. M. W. Haney, M. P. Christensen, P. Milojkovic, J. Ekman, P. Chandramani, R. Rozier, F. Kiamilev, Y. Liu, and M. Hibbs-Brenner, "Multichip free-space global optical interconnection demonstration with integrated arrays of vertical-cavity surface-emitting lasers and photodetectors," Applied Optics, Vol. 38, pp. 6190-6200, 1999.
10. E. M. Strzelecka, D. A. Louderback, B. J. Thibeault, G. B. Thompson, K. Bertilsson, and L. A. Coldren, "Parallel free-space optical interconect based on arrays of vertical-cavity lasers and detectors with monolithic microlenses," Applied Optics, Vol. 37, pp. 2811-2821, 1998.
11. R. Wong, A. D. Rakic, and M. L. Majewski, "Design of microchannel free-space optical interconnects based on vertical-cavity surface-emitting laser arrays," Applied Optics, Vol. 41, pp. 3469-3478, 2002.
12. R. Wong, A. D. Rakic, and M. L. Majewski, "Analysis of lensless free-space optical interconnects based on multi-transverse mode vertical-cavity-surface-emitting lasers," Optics Communications, Vol. 167, pp. 261-271, 1999.
13. X. Zheng, P. J. Marchand, D. Huang, and S. C. Esener, "Free-space parallel multichip interconnection system," Applied Optics, Vol. 39, pp. 3516-3524, 2000.

14. N. S. Petrovic and A. D. Rakic, "Modeling diffraction in free-space optical interconnects by the mode expansion method," Applied Optics, Vol. 42, pp. 5308-5318, 2003.
15. X. Zheng, P. J. Marchand, D. Huang, O. Kibar, and S. C. Esener, "Cross talk and ghost talk in a microbeam free-space optical interconnect system with vertical-cavity surface-emitting lasers, microlens, and metal-semiconductor-metal detectors," Applied Optics, Vol. 39, pp. 4834-4841, 2000.
16. F. Lacroix, M. Châteauneuf, X. Xue, and A. G. Kirk, "Experimental and numerical analyses of misalignment tolerances in free-space optical interconnects," Applied Optics, Vol. 39, pp. 704-713, 2000.
17. F. F. Tsai, C. J. O'Brien, N. S. Petrovic, and A. D. Rakic, "Analysis of optical channel cross talk for free-space optical interconnects in the presence of higher-order transverse modes," Applied Optics, Vol. 44, pp. 6380-6387, 2005
18. F. F. Tsai, C. J. O'Brien, N. S. Petrovic, and A. D. Rakic, "Analysis of novel array geometry for free-space optical interconnects with improved signal-to-noise ratio," Applied Optics, to be accepted for publication, 2006
19. A. E. Siegman, *Lasers,* University Science Books, Sausalito, Cal, 1986.